

MOVING HEAT SOURCES IN A HALF SPACE: EFFECT OF SOURCE GEOMETRY

Mohsen Akbari*, David Sinton^o, Majid Bahrami*

*Mechatronic System Engineering School of Engineering Science,
Simon Fraser University, Surrey, BC, V3T 0A3.

^oDepartment of Mechanical Engineering,
University of Victoria, Victoria, BC, V8W 2Y2, Canada.

Abstract

The time dependent temperature distribution due to a moving plane heat source of hyperelliptical geometry is analytically studied in this work. The effect of the heat source shape is investigated starting from the general solution of a moving heat source on a half space. Selecting the square root of the heat source area as a length scale, it is observed that the temperature distribution becomes a weak function of the heat source shape. Variation of temperature field with respect to the source aspect ratio, velocity and depth is studied. The analysis presented in this work is valid for both transient and steady-state conditions. In addition, the hyperellipse formulation provided here covers a wide range of shapes including star, rhombic, ellipse, circle, square, rectangle and rectangle with rounded corners.

1 Introduction

Stationary and moving plane heat source analysis have application in several manufacturing processes such as metal cutting, spot welding, laser cutting/surface treatment (using CO₂ or Argon lasers) as well as tribological applications including ball bearing and gear design [1-5]. Temperature profile and the rate of cooling at and near the surface can affect the metallurgical microstructures, thermal shrinkage, thermal cracking, hardness distribution, residual stresses and heat affected zones of the material [6]. Knowing temperature distribution in tribological applications due to frictional heat generation is required to minimize thermal related problems such as lubricant break down [7].

In the area of microfluidics for biomedical and lab-on-chip applications, accumulation of DNA molecules has

been demonstrated by applying large temperature gradients provided by a laser beam [8]. This accumulation is described to be a result of thermophoresis phenomena and free convection [8]. In thermophoresis, molecules are moved by a thermal gradient. Combining thermophoresis and electrophoresis effects, Duhr and Braun [9] developed a new method for molecular focusing.

In many applications the size of the heat source compared to the conducting body is small enough to assume a heat source on a half space. Temperature distribution in the medium can then be predicted with the solution of the Laplace's equation and appropriate boundary conditions for various source shapes.

A direct solution of Laplace's equation, to find a solution for a plane heat source of various shapes and distributions, may not be simple and straightforward. In some cases, even if the PDE can be solved, it is still not certain whether it would be possible to determine the

relevant unknown coefficients in the final solution. One well-known example is the stationary continuous point source on a half space, where it is impossible to mathematically apply the boundary conditions at the heat source. Hence other methods have been developed to overcome these complexities. Using the concept of instantaneous point source introduced by Carslaw and Jaeger [10], is a common approach to determine transient temperature distribution within an infinite/semi-infinite body. Temperature distribution due to a continuous point source can be obtained by integrating the solution of instantaneous point source with respect to time [10]. Letting time goes to infinity, the solution yields to the steady point source, which corresponds to the well-known source solutions of hydrodynamics [10]. Integrating the solutions for point sources with regard to appropriate space variables, solutions can be obtained for instantaneous and/or continuous line, plane, spherical surface, and cylindrical surfaces [10-16].

Jaeger [16] and Rosenthal [17] used the instantaneous point source solution to find the temperature distribution due to a moving heat source within an infinite body. Applying the same method, Peak and Gagliano [18], found a transient solution to determine the temperature distribution for laser drilled holes in ceramic substrate materials. They [18] considered a circular heat source and found the temperature profile in the form of double integrals, which cannot be solved analytically. The same approach has been used by Zubair and Chaudhry [19] for a moving line source with time variable heat flow rate, and Terauchi et al. [20] for moving circular and rectangular plane sources. In the later one [20], the effect of different heat flux distributions has been investigated for the quasi-steady condition. They showed that for a constant value of heat flow rate, the peak in the temperature profile is the highest for parabolic heat flux rather than uniform and/or Gaussian profiles. Muzychka and Yovanovich [7] developed a model to predict the thermal resistance of non-circular moving heat sources by combining asymptotic solutions of very fast moving, and stationary heat sources. They [7] showed that the dimensionless thermal resistance, which is directly proportional to the maximum surface temperature, is a weak function of the heat source shape if the square root of the contact area is used as a characteristic length. However, their solution is only valid for quasi-steady condition. Several other researchers have used the point source solution in the quasi-steady condition to study the moving line and plane source with different shapes on a half space [21-26]. Recently, Hou and Komandouri [6] used this approach and reported a general solution for transient temperature distribution of a moving plane source in a half space. Their solution includes a triple integral; one over time and two over the heat source surface. The time integral is in the form of the well known Macdonald's function. They [6] solved the integrals

numerically for various heat source shapes including elliptic, circular, rectangular and square surfaces. More recently, using almost the same method, Kou and Lin [25] found a three dimensional solution for the rectangular shaped moving heat source.

The transient and steady state temperature distribution due to a moving plane heat source is the focus of present study. Main objectives of this work are: (a) to examine the effect of heat source shape on the temperature distribution within a half space, and (b) to gain detailed understanding of temperature distribution due to a moving plane source of arbitrary shape. We considered a hyperellipse since it covers a wide variety of shapes including star shape, rhombic, ellipse, circle, rectangle, square, and line source. Results of the present analysis may ultimately be applied to develop a novel technique for separation of different molecules or predict channel dimensions in laser micromachining for microfluidics purposes.

2 Theory

The classical approach introduced by Carslaw and Jaeger [10] is used in this work. Starting from the solution of an instantaneous point source, transient temperature distribution in a half space due to a moving point source is obtained. General transient solution of the moving plane source can then be found using the superposition of the solutions of the point sources over the heat source surface [6].

2.1 Instantaneous point source

If heat is released at time, $t = 0$ at point $P(x, y, 0)$ on a half space with initial temperature of T_0 as shown in Figure 1, the Laplace's equation in the Cartesian coordinate has the following form

$$\frac{\partial^2 \theta}{\partial x^2} + \frac{\partial^2 \theta}{\partial y^2} + \frac{\partial^2 \theta}{\partial z^2} = \frac{1}{\alpha} \frac{\partial \theta}{\partial t} \quad (1)$$

where $\theta = T - T_0$ is the temperature rise, $\alpha = k/\rho c_p$ is the thermal diffusivity of the half space, k , ρ , and c_p are the thermal conductivity, density and heat capacity of the half space, respectively. Thermal boundary conditions are: initial temperature in regions remote from the source, i.e. $\theta = 0$, when $R = \sqrt{x^2 + y^2 + z^2} \rightarrow \infty$, and the prescribed amount of released heat, $Q [J]$, through the point source. All points except the point source are assumed to be adiabatic; i.e. $(d\theta/dz)_{z=0} = 0$. Equation (1) is satisfied by the following temperature distribution [10]

$$\theta(t) = \frac{Q e^{-\left(\frac{R}{4\alpha t}\right)}}{4\rho c_p (\pi\alpha)^{3/2}} \quad (2)$$

where $R = \sqrt{(x - \chi)^2 + (y - \gamma)^2 + z^2}$ is the distance from the point source. It can be shown that temperature at a point distance of R from the source has its maximum value at time $t = R^2/6\alpha$. Time dependent temperature distribution of a continuous point source can then be obtained by integrating Eq. (2) from the initial to present time. The final result has the following form [10]

$$\theta(t) = \frac{\dot{Q}}{2\pi\alpha R} \operatorname{erfc}\left(\frac{R}{\sqrt{4\alpha t}}\right) \quad (3)$$

where $R = \sqrt{(x - \chi)^2 + (y - \gamma)^2 + z^2}$. For steady state condition, as $t \rightarrow \infty$, Eq.(3) reduces to $\theta = \dot{Q}/2\pi\alpha R$ which can also be obtained by applying the Fourier's equation in a half space [11].

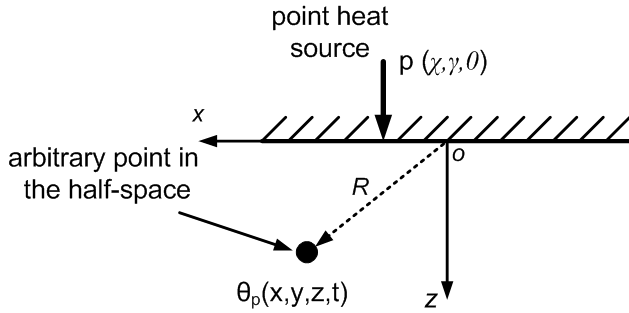


Figure 1. Schematic of the stationary point source.

2.2 Moving point source

If the point source shown in Figure 1 moves with a constant velocity of U in the x -direction, temperature distribution at time, t , due to the amount of heat released when the source was at $(Ut', \gamma, 0)$ is

$$d\theta = \frac{\dot{Q}}{4\rho c_p (\pi\alpha)^{3/2}} \frac{e^{-\left\{\frac{(x-Ut')^2 + (y-\gamma)^2 + z^2}{4\alpha(t-t')}\right\}}}{(t-t')^{3/2}} dt' \quad (4)$$

where \dot{Q} [W] is the amount of heat flow rate. Integrating Eq. (4) over time, the following expression for temperature distribution in a half space can be obtained

$$\theta(t) = \frac{\dot{Q}}{4\rho c_p (\pi\alpha)^{3/2}} \int_0^t \frac{e^{-\left\{\frac{(x-Ut')^2 + (y-\gamma)^2 + z^2}{4\alpha(t-t')}\right\}}}{(t-t')^{3/2}} dt' \quad (5)$$

Letting $\tau = t - t'$ and for constant heat flow rate, \dot{Q} , and properties, Eq. (5) yields

$$\theta(t) = \frac{\dot{Q}}{4\rho c_p (\pi\alpha)^{3/2}} \int_0^t \frac{e^{-\left\{\frac{(x-Ut+U\tau)^2 + (y-\gamma)^2 + z^2}{4\alpha\tau}\right\}}}{\tau^{3/2}} d\tau \quad (6)$$

Denoting $X = (x - Ut)$ which is the moving coordinate attached to the heat source at time t , Eq. (6) reduces to

$$\theta(x, y, z, t, U) = \frac{\dot{Q} e^{-\frac{UX}{2\alpha}}}{4\rho c_p (\pi\alpha)^{3/2}} \int_0^t \frac{e^{-\left[\frac{R^2}{4\alpha\tau} - \frac{U^2\tau}{4\alpha}\right]}}{\tau^{3/2}} d\tau \quad (7)$$

where $R = \sqrt{X^2 + y^2 + z^2}$ is the distance from the point source in the moving coordinate. By changing variables, $\eta = U^2\tau/4\alpha$ Eq. (7) in dimensionless form becomes

$$\theta^*(x^*, y^*, z^*, Fo, Pe) = \frac{e^{-PeX^*} Pe}{4\pi^{3/2}} I_t \quad (8)$$

where $x^* = x/L$, $y^* = y/L$, $z^* = z/L$, $Fo = \alpha t/L^2$, $Pe = UL/2\alpha$, $R^* = R/L$, $\beta = Pe^2 Fo$, $\epsilon = PeR^*/2$, $\theta^* = \theta kL/\dot{Q}$ and I_t is the time integral term

$$I_t = \int_0^\beta \frac{e^{-\left(\frac{\epsilon^2}{\eta} + \eta\right)}}{\eta^{3/2}} d\eta \quad (9)$$

In Eq. (8), L is the length scale. Selection of this characteristic length is an arbitrary choice and will not affect the final solution. However, an appropriate length scale leads to more consistent results, especially when general geometry is considered. A circular heat source is fully described with its diameter, thus the obvious length scale is the diameter (or radius). For non-circular sources, the selection is not as clear. Yovanovich [27] introduced the square root of area as a characteristic length scale for heat conduction and convection problems. Therefore, in this study, \sqrt{A} is selected consistently as the length scale throughout the analysis.

Peclet number Pe , appears in Eq. (8) is the ratio of heat source velocity to the amount of heat diffuses into the half space, and Fourier number, Fo is the dimensionless time.

Hou and Komanduri [6] reported that the time integral of Eq. (9) is very similar to the modified Bessel function of the second kind. However, they did not provide a close form for this integral and solved numerically. Effort has been made in this work to find an exact solution for this integral. A close form has been found as follows

$$I_t = \frac{\sqrt{\pi}}{PeR^*} (I_1 + I_2) \quad (10)$$

where

$$I_1 = e^{PeR^*} \operatorname{erfc} \left(\frac{R^*}{2\sqrt{Fo}} + Pe\sqrt{Fo} \right) \quad (11)$$

$$I_2 = e^{-PeR^*} \operatorname{erfc} \left(\frac{R^*}{2\sqrt{Fo}} - Pe\sqrt{Fo} \right)$$

Note that in the limiting case, when $Fo \rightarrow \infty$ (i.e. the quasi-steady condition), Eq. (8) yields

$$\theta^* = \frac{e^{-Pe(R^*+X^*)}}{2\pi R^*} \quad (12)$$

which is the well-known solution of a moving point source in a half space [10]. Equation (8) is a general solution for a moving point source that gives the temperature field within a half space at any time.

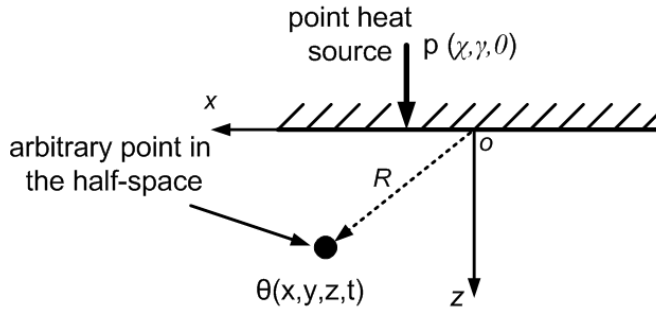


Figure 2. Schematic of arbitrary shape moving plane source.

2.3 Moving plane source

Consider a plane moving source, having an arbitrary shape as shown in Figure 2. The solution of the moving point source can be extended to plane heat source by superimposing the temperature rise due to each moving infinitesimal element. Hence

$$\theta^* = \frac{Pe}{4\pi^{3/2}} \int_{\chi_1^*}^{\chi_2^*} \int_{f(\chi_1^*)}^{f(\chi_2^*)} e^{-Pe(X^*-\chi^*)} I_t d\gamma^* d\chi^* \quad (13)$$

where $R^* = \sqrt{(X^* - \chi^*)^2 + (y^* - \gamma^*)^2 + z^{*2}}$, $\theta^* = \theta k / \dot{q} L$ and I_t is the time integral defined in Eqs. (10) and (11). A closed solution for Eq. (11) has not been found even for simple geometries such as an ellipse or rectangle and it is typically solved numerically.

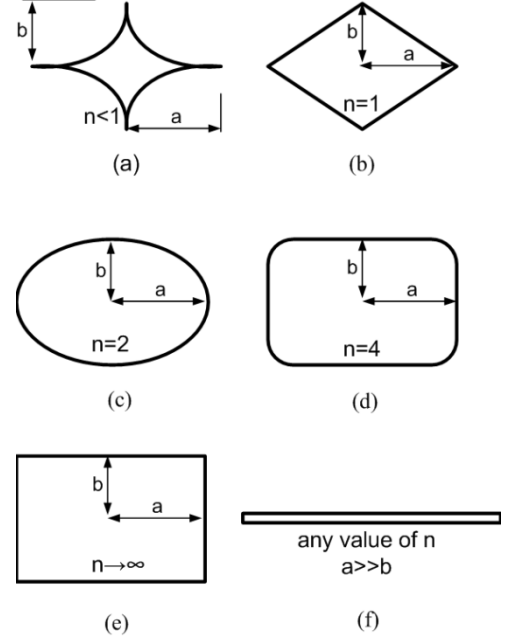


Figure 3. Hyperellipse as a general symmetric geometry, (a) star shape ($n < 1$), (b) rhombic ($n = 1$), (c) ellipse ($n = 2$), (d) rectangle with round corners ($n = 4$), (e) rectangle ($n \rightarrow \infty$), (f) line (any value of n but $a \gg b$).

3. Results and discussion

The general solution obtained in Eq. (13) is solved for a hyperelliptical heat source represented by

$$\left(\frac{x}{a}\right)^n + \left(\frac{y}{b}\right)^n = 1 \quad (14)$$

where a and b are the major and minor axis, respectively and n defines the shape of the geometry. We considered hyperellipse heat source as a general geometry since it covers a wide variety of shapes. As shown in Figure 3, star shape, rhombic, ellipse, round corner rectangle, and rectangle can be obtained for $n < 1$, $n = 1$, $n = 2$, $n = 4$ and $n \rightarrow \infty$, respectively. By changing the aspect ratio, i.e. $\varepsilon = b/a$, circular, square and line heat sources may be obtained as well.

Using Eq. (12) and the definition of aspect ratio $\varepsilon = b/a$, Eq. (13) becomes

$$\theta^* = \frac{Pe}{4\pi^{3/2}} \int_{-a^*}^{a^*} \int_{-\varepsilon a^*}^{\varepsilon a^*} \left[1 - \left(\frac{\chi^*}{a^*}\right)^n \right]^{1/n} e^{-Pe(X^*-\chi^*)} I_t d\gamma^* d\chi^* \quad (15)$$

An in house computational code is developed in Maple 11 [28] to solve Eq. (15) numerically. Uniform heat flux is considered in this work. To ensure that for different

geometries the same heat flow rate enters the half space, source area is assumed to remain constant.

Dimensionless temperature distribution on the major axis of an elliptical moving heat is plotted Figure 4 for $z^* = 0$. Used values of Peclet number and heat source aspect ratio ε are listed in Table 1. Horizontal axis is in the absolute coordinate. It can be observed that:

- Since the source is moving, there is no symmetry in the temperature distribution in the moving direction. Temperature peak tends towards the moving direction while the points on the footprint of the heat source are still cooling down and forming a tail in the temperature profile.
- Temperature gradient at the front edge is larger compared to the rear edge; thus, more heat is transferred to the half space through this edge. As a result, maximum temperature occurs closer to the rear edge of the heat source. Similar results can be observed in the temperature distributions in the works of Hou and Kumanduri [6] and Terauchi et al. [20].
- Temperature peak rapidly approaches steady value; however the temperature profile needs some more time to reach the quasi-steady condition. The reason is that the points on the trail of the heat source are still cooling down while the peak temperature moves with the heat source.

Table 1. Typical values used in Figures 4 and 5.

Parameter	Value
n	2
Pe	11.15
$\varepsilon = b/a$	0.5

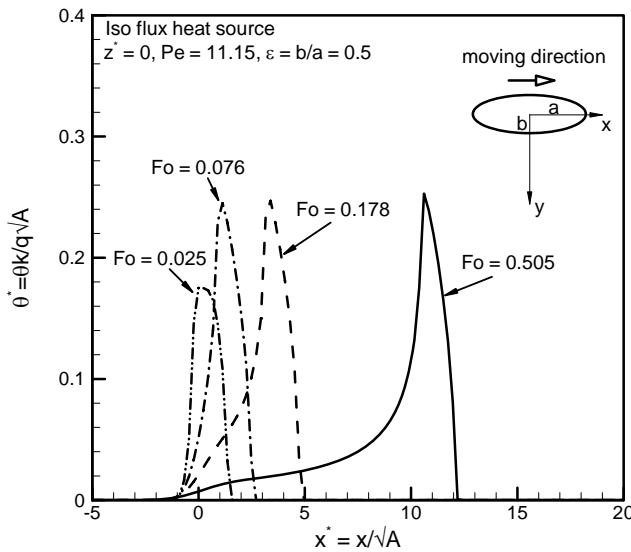


Figure 4. Transient dimensionless temperature distribution on the elliptical moving heat source surface.

Values of maximum temperature on the heat source surface as a function of the Fourier number, Fo , is plotted in Figure 5. The same values listed in Table 1 are used for the Peclet number and aspect ratio for different heat source geometries. The effect of various geometrical shapes have been investigated by changing the shape parameter, n , in the range of $0.5 \leq n \leq \infty$. As can be seen, maximum temperature is a weak function of shape. For $n \geq 1$, the effect of the heat source shape is negligible; less than 1%. The difference between the elliptical and star shape geometry i.e. $n = 0.5$, is approximately 4%. For all geometries, maximum temperature increases rapidly and reaches 95% of its steady-state value at a Fourier number, Fo^* . This number for the typical values of Pe and ε listed in Table 1 is $Fo^* \approx 0.07$.

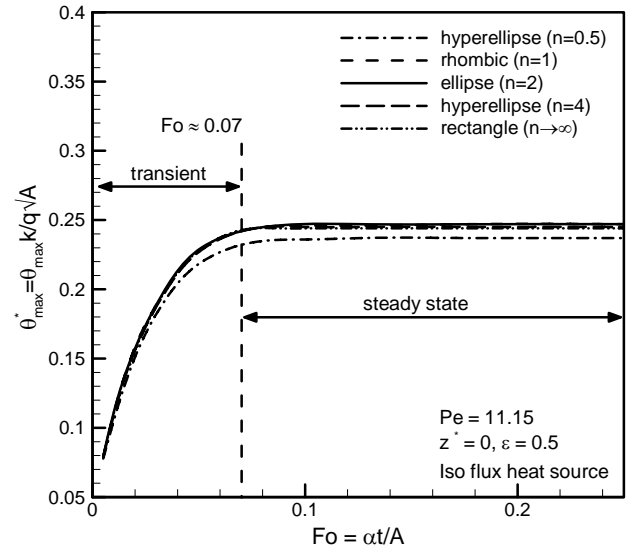


Figure 5. Maximum temperature as a function of the Fourier number for different geometries.

4. Parametric study

Present analysis can be used to investigate the influence of important parameters on the temperature distribution. In the previous section, the effect of the Fourier number, Fo , on the temperature distribution and maximum temperature of the heat source has been investigated. It has been observed that the heat source shape, (i.e. n) in Eq. (15) has a small effect on the variation of maximum temperature with time. In this section, the effect of Peclet number, Pe , heat source aspect ratio, ε and shape parameter, n on the temperature field within the half space are presented.

4.1. Effect of shape parameter, n

As describe earlier, n in Eq. (14) defines the type of the hyperelliptical geometry. By changing this parameter, different geometries such as star shape, rhombic, ellipse and rectangular shapes can be obtained. Table 2 presents the maximum dimensionless temperature for a range of shape parameter, n and three aspect ratios of $\varepsilon = 0.1, 0.5$ and 1 . Results are also plotted in Figure 6 for two typical aspect ratios of $\varepsilon = 0.1$ and 0.5 . The solid lines represent the mean values. As can be seen, the effect of shape parameter on the maximum temperature is very small (within $\pm 2\%$). In most cases deviation from the mean value is less than $\pm 1\%$. As a result, maximum temperature can be considered to be independent of the heat source geometry.

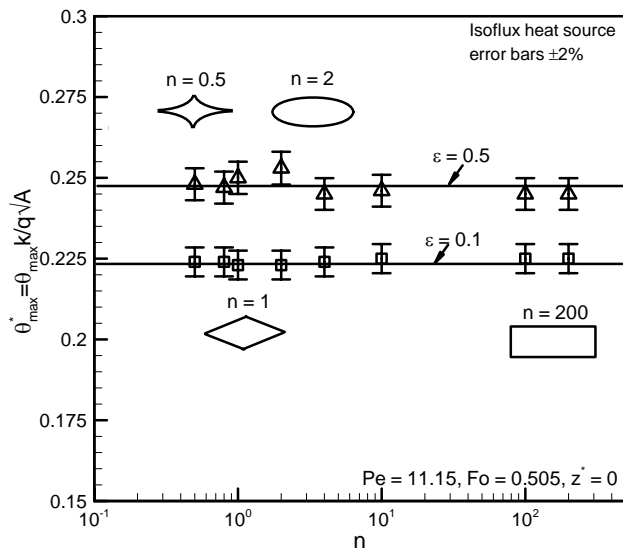


Figure 6. Maximum temperature vs. shape parameter, n .

Table 2. Maximum dimensionless temperature, θ_{max}^* for moving isoflux hyperellipse heat sources, $Pe = 11.15$ and $Fo = 0.505$.

n	$\varepsilon = 0.1$	$\varepsilon = 0.5$	$\varepsilon = 1$
0.5	0.224	0.248	0.228
0.8	0.224	0.247	0.229
1	0.223	0.250	0.231
2	0.223	0.253	0.232
4	0.224	0.245	0.227
10	0.225	0.246	0.225
100	0.225	0.245	0.224
200	0.225	0.245	0.224

4.2. Effect of aspect ratio

The temperature distribution due to a moving elliptical heat source on the surface of a half space is plotted in Figure 7. A typical Peclet number of $Pe = 11.15$ is used for the quasi-steady condition. The effect of source aspect ratio on the temperature field is investigated. Smaller aspect ratios mean that the heat source is more stretched in the moving direction. Therefore, a flatter temperature distribution can be observed. At the limiting case, where $\varepsilon \rightarrow 0$, the plane heat source becomes an isothermal line source with an infinite length.

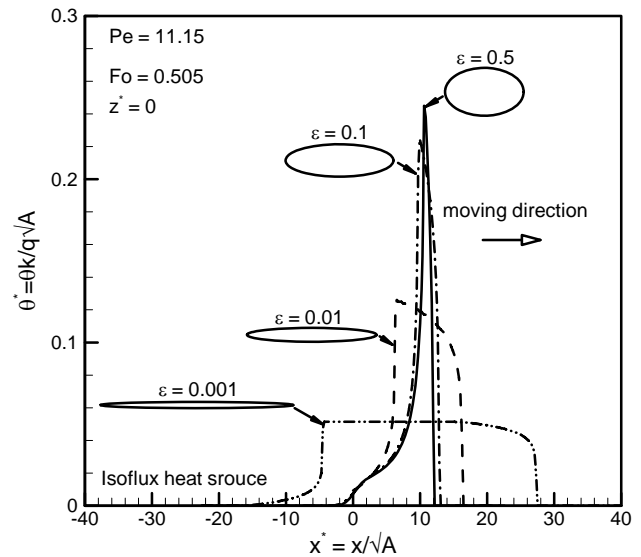


Figure 7. Variation of temperature on the heat source surface for an elliptical shape source.

Due to sharper temperature gradient at the front edge, more heat is transferred through this edge. However, since the major axis is much larger than the minor axis for smaller aspect ratios, most of the heat tends to transfer in the perpendicular direction of the heat source motion; thus heat transfer through the front and rear edges becomes negligible, and the maximum temperature decreases.

Figure 8, shows the variation of maximum temperature with aspect ratio on the surface of the elliptical and rectangular heat sources. As can be seen, the maximum temperature increases with the aspect ratio having a maximum at $\varepsilon \approx 0.45$. For higher values of the aspect ratio, the effect of the front and rear edges becomes important, while the heat transfer in perpendicular direction decreases. As a result of low temperature gradients, less heat is dissipated from the rear edge; as a result, maximum temperature increases with aspect ratio. After a particular aspect ratio (here $\varepsilon \approx 0.45$), the minor axis becomes comparable with the major axis, heat transfer in the moving direction increases and the maximum temperature decreases.

It is also beneficial to investigate the effect of heat source aspect ratio on the position of temperature peak, X_{max}^* . The maximum temperature always occurs on the major axis of the heat source since the temperature distribution is symmetrical in its perpendicular direction. Due to the unsymmetrical nature of the temperature distribution in the moving direction, the peak temperature position is closer to the rear edge of the heat source. Variation of peak temperature position in the moving coordinate, X_{max}^* , as a function of source aspect ratio is plotted in Figure 9 for the elliptical heat source. As shown, when the aspect ratio increases, the location of the maximum temperature becomes closer to the center of the heat source. For very small the aspect ratios, this location becomes independent of aspect ratio. Note that the limiting case of $\varepsilon \rightarrow 0$ is an isothermal line source with infinite length.

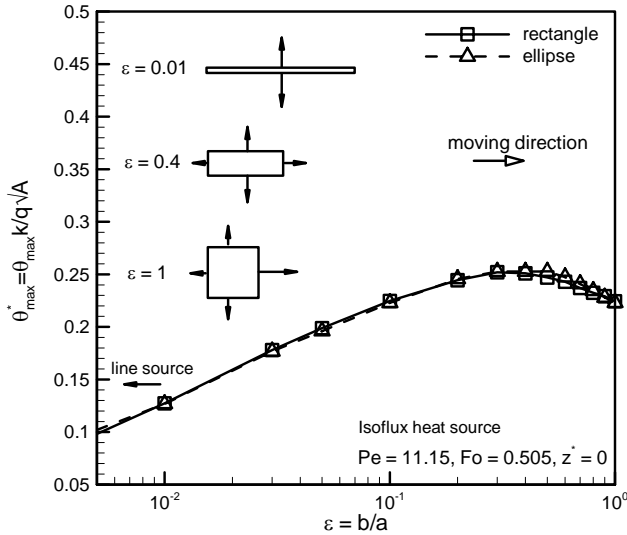


Figure 8. Maximum temperature as a function of aspect ratio for different geometries.

4.3. Effect of heat source velocity

Effect of the heat source speed on the temperature distribution of a half space is addressed in various applications. For instance, Sun et al. [1] and Klank et al. [2], reported that the depth of the microchannels fabricated with a CO₂ laser decreases significantly with the increase of the beam speed for a constant power. Figure 10 quantitatively shows the variation of channel depth when laser beam speed varies linearly and power is constant. As can be seen, channel depth rapidly increases for slower beam speeds. For higher speeds, variation of the beam velocity does not have significant effect on the channel depth. This is due to the fact that when the heat

source moves at a higher speed, it spends a shorter time at each spot, and consequently less heat is absorbed by the material.

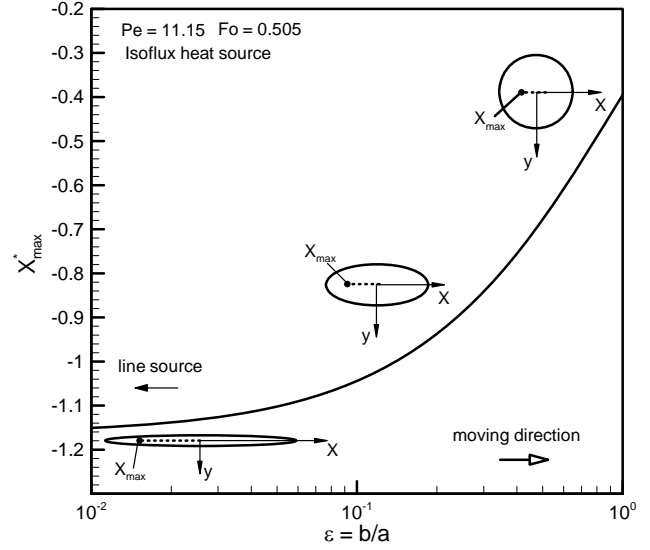


Figure 9. Variation of maximum temperature location as a function of the aspect ratio for an elliptical heat source.

Variation of maximum temperature with Peclet number is plotted in Figure 11. Since the effect of geometry has been observed to be negligible, the elliptical heat source is considered with the typical aspect ratio of $\varepsilon = 0.5$. Two asymptotes can be recognized in Figure 11: (a) stationary heat source ($U \rightarrow 0$), and (b) very fast moving heat source ($U \rightarrow \infty$).

Yovanovich et al. [21] developed a model to predict steady-state thermal constriction resistance of planar contact areas of arbitrary shape with constant heat flux. Hyperelliptical geometry was investigated in their work and thermal resistance based on the average and maximum source temperatures was reported. According to the definition of thermal resistance based on the maximum temperature, $\theta_{max}^* = \hat{R}^*$ where $\hat{R}^* = \hat{R}k\sqrt{A}$ and $\hat{R} = \theta_{max}/\dot{q}A$. For $\varepsilon = 0.5$, maximum temperature has the value of 0.5455, after interpolation.

For a very fast moving heat source, Muzychka and Yovanovich [7], proposed a model for the elliptical shape. Maximum temperature can be obtained from the following relationships [7]:

$$\theta_{max}^* = 1.2 \sqrt{\frac{\varepsilon}{Pe}} \quad (16)$$

Combining the stationary and very fast moving heat source solutions and using the Churchill and Usagi method [29], the following correlation has been developed for an elliptical heat source

$$\theta_{max}^* = \frac{\sqrt{\varepsilon}}{(6.52\varepsilon\sqrt{\varepsilon} + 0.58Pe\sqrt{Pe})^{1/3}} \quad (17)$$

The solid line in Figure 11 represents Eq. (17) and the symbols are the numerical results of present analysis, obtained from Eq. (15). It can be seen that Eq. (17) can predict the variation of maximum temperature on the heat source surface with good accuracy (average error is 6.5%). Since maximum temperature can be considered to be independent of the source geometry, Eq. (17) can be used for other geometries as well.

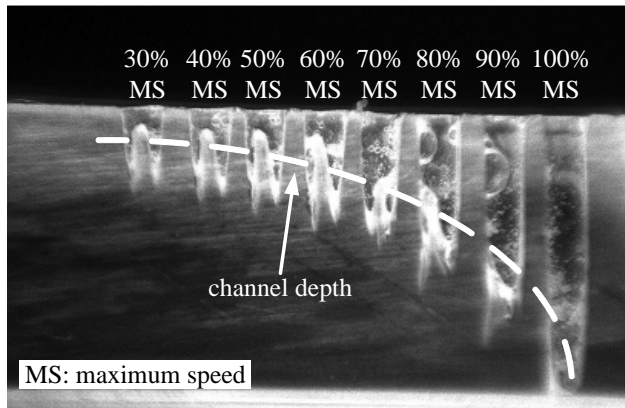


Figure 10. Variation of channel depth with beam speed. Channels were engraved in PMMA using a CO2 laser machine at the power of 60W (Universal laser Microsystems Inc., USA).

4.4. Effect of depth

Temperature distribution under the surface of the heat source is important in many manufacturing applications [1-6]. For instance, in laser micromachining, channel geometry depends on the temperature distribution at and near the surface of spot. Thus, it is desirable to know the temperature distribution of both on and under the heat source surface.

Figure 12 shows the dimensionless steady-state temperature distribution on the major axis of an elliptical moving heat source surface in different depths. It is clear from Figure 12 that the maximum temperature has a lag in deeper positions because of the penetration time. The time required for a part of the body located at the depth of z from the heat source to sense the heat source is z^2/α .

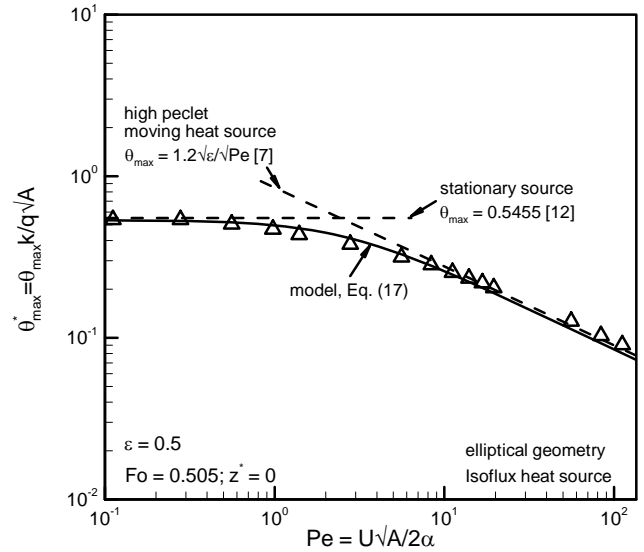


Figure 11. Variation of maximum temperature on the surface of an elliptical moving heat source vs. Peclet number. Solid line represents the developed correlation, i.e. Eq. (17) and the symbols are the numerical results of obtained from Eq. (15).

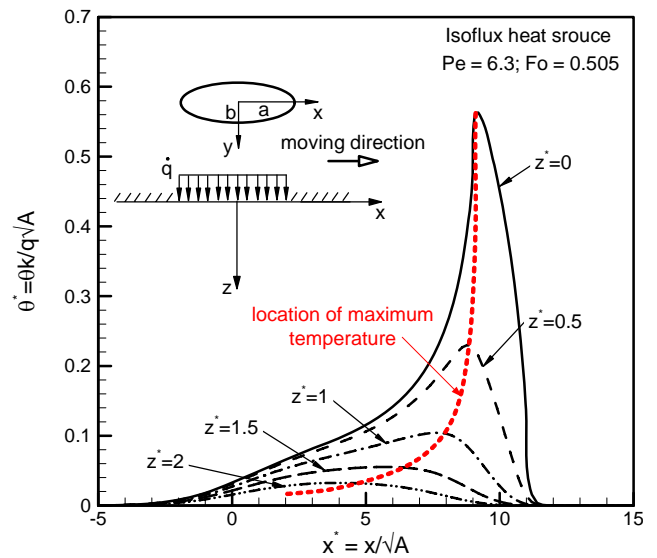


Figure 12. Temperature distribution in different depths for an elliptical heat source.

Maximum temperature as a function of dimensionless depth is plotted in Figure 13 for three heat source geometries: rhombic, ellipse and rectangle. It can be seen that temperature drops rapidly at points near the heat source surface followed by a gradual change with increasing depth. This temperature gradient It can also be

observed that the effect of heat source shape on the maximum temperature is small and can be neglected.

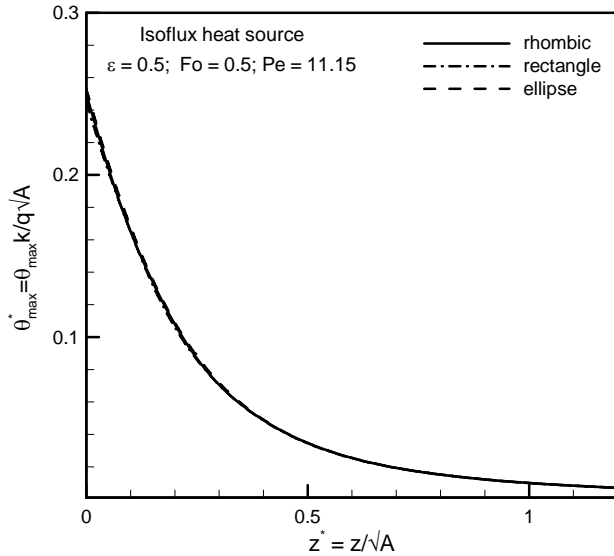


Figure 13. Variation of maximum temperature with depth for moving heat source of various shapes.

4. Summary and conclusion

Using the general solution of a moving heat source in a half space and the superposition technique, time dependent temperature distribution due to moving the plane heat source of hyperelliptical geometry was analytically investigated. The major focus of this work was to study the effect of a heat source shape on the temperature distribution on and under the surface of the heat source. We considered a hyperelliptical heat source as a general geometry since it covers a wide variety of shapes including: rhombic, elliptical, circular, rectangular, and square. Following results were obtained through the present analysis:

- As a result of the heat source motion, unsymmetrical temperature field is formed on both the surface and deep into the half space.
- Since the temperature gradient is larger in the front edge of the heat source, the location of the maximum temperature is closer to the rear edge.
- The peak temperature reaches the steady-state value rapidly; however the temperature profile requires more time to reach the quasi-steady condition.
- The temperature field is a weak function of source shape. However, the aspect ratio has a significant effect on the maximum temperature, especially for small values.
- When aspect ratio increases, the location of the maximum temperature approaches the center of heat

source. For very small aspect ratios, this location no longer varies and the solution becomes similar to the case of a line source with infinite length.

- The source velocity has significant effect on the temperature field. The higher the speed of the source, the lower the maximum temperature.
- The temperature decreases with distance into the half space and the maximum temperature does not occur in the same location as for the surface of the heat source.

For future works, more geometry will involve in the solution with different types of heat flux distribution.

Acknowledgment

The authors gratefully acknowledge the financial support of the Natural Sciences and Engineering Research Council of Canada, NSERC.

Nomenclature

A	=	Heat source surface area, m^2
a	=	Hyperellipse major axis, m
b	=	Hyperellipse minor axis, m
c_p	=	Heat capacity, $J/kg.K$
Fo	=	Fourier number, at/A
k	=	Thermal conductivity, $W/m.K$
Pe	=	Peclet number, $UL/2\alpha$
Q	=	Released energy, J
\dot{Q}	=	Released energy per unit time, W
\dot{q}	=	Released energy per unit time per unit area, W/m^2
U	=	Heat source speed, m/s
T	=	Temperature at any arbitrary point, K or $^\circ C$
T_{ref}	=	Reference temperature, K or $^\circ C$

Greek

α	=	Thermal diffusivity, m^2/s
ρ	=	Density, kg/m^3

References

- [1] Sun, Y., Kwok, Y.C., Nguyen, N.T., 2006, "Low pressure, high temperature thermal bonding of polymeric microfluidic devices and their applications for electrophoretic", *J. Micromech. and Microeng.* 16, pp. 1681-1688.
- [2] Kricka, L.J., Fortina, P., Panaro, N.J., Wilding, P., Amigo, G.A., Becker, H., 2002, "Fabrication of plastic microchips by hot embossing", *Lab. Chip* 2, pp. 1-4.
- [3] Halling, J., 1975, *Principles of Tribology*, McMillan Education Ltd.
- [4] Williams, J.A., 1994, *Engineering Tribology*, Oxford University Press.

- [5] Winer, W.O., Chen H.S., 1980, "Film thickness, contact stress and surface temperatures", in *Wear Control Handbook*, ASME Press, New York, pp. 81-141.
- [6] Hou, Z.B., Komanduri, R., 2001, "General solutions for stationary/moving plane heat source problems in manufacturing and tribology", *Int. J. Heat and Mass Transfer* 43, pp. 1679-1698.
- [7] Muzychka, Y.S., Yovanovich, M.M., 2001, "Thermal resistance models for non-circular moving heat sources on a half space", *Journal of Heat Transfer*, ASME Trans. 123, pp. 624-632.
- [8] Braun, D., Libchaber, A., 2002, "Trapping of DNA by thermophoretic depletion and convection", *Physical Review Letter* 89 (18), pp. 188103.
- [9] Duhr, S., Braun, D., 2006, "Optothermal molecule trapping by opposing fluid flow with thermophoretic drift", *Physical Review Letter* 97 (18), pp. 038103.
- [10] Carslaw, H.S., Jeager, J.C., 1959, *Conduction of heat in solids*, Oxford University Press.
- [11] Yovanovich, M.M. 1975, "Thermal constrict resistance of contacts on a half space: integral formulation, *AIAA Prog. in Astro. and Aeronautics: Thermophysics and Space Craft Control* 35, R. G. Hering, ed., MIT Press, Cambridge, MA, pp. 265-291.
- [12] Yovanovich, M.M., Burde, S.S., and Thomson J.C., 1977, "Thermal constriction resistance of arbitrary planar contacts with constant heat flux", *AIAA Prog. in Astro. and Aeronautics: Thermophysics and Space Craft Control* 56, A.M. Smith, ed., pp. 127-139.
- [13] Yovanovich, M.M., Negus, K.J., Thomson, J.C., 1984 "transient temperature rise of arbitrary contacts with uniform flux by surface element methods, *AIAA 22nd Aerospace Science Meeting*, Reno, NV, pp. 1-7.
- [14] Negus, K.J. and Yovanovich, M.M., 1989, Transient temperature rise at surface due to arbitrary contacts on half space, *Transaction of CSME* 13 (1/2), pp. 1-9.
- [15] Yovanovich, M.M., 1997, Transient spreading resistance of arbitrary Isoflux contact areas: development of a universal time function, 33rd Annual AIAA Thermophysics Conference, Atlanta, GA.
- [16] Jeager, J.C., 1942, "Moving sources of heat and temperature at sliding contacts", *Proceeding of Royal Society*, New South Wales, 76, pp. 203-224.
- [17] Rosenthal, D., 1946, "The theory of moving sources of heat and its application on metal treatment", *ASME Trans.* 68, pp. 849-866.
- [18] Peak, U., Gagliano, F.P., 1972, "Thermal analysis of laser drilling processes", *IEEE J. of Quantum Electronics* 2, pp. 112-119.
- [19] Zubair, S. M., Chaudhry, M. A., 1996, "Temperature solutions due to time-dependent moving line heat sources", *Heat and Mass Transfer* 31, pp. 185-189.
- [20] Terauchi, Y., Nadano, H., 1984, "On temperature rise caused by moving heat sources", *Bull. of JSME* 27, No 226, pp. 831-838.
- [21] Weichert, R., Schonert, K., 1978, "Temperature distribution produced by a moving heat source", *Q. J. Mech. Appl. Math.* XXXI, pp. 363-379.
- [22] Zhang, H.J., 1990, "Non-quasi-steady analysis of heat conduction from a moving heat source", *ASME J. Heat Transfer* 112, pp.777-779.
- [23] Tian, X., Kennedy, F.E., 1994, "Maximum and average flash temperature in sliding contacts", *ASME J. Tribology* 116, pp. 167-174.
- [24] Zeng, Z., Brown, M.B., Vardy, A.E., 1997, "On moving heat sources", *Heat and Mass Transfer* 33, pp. 41-49.
- [25] Kou, W.L., Lin, J.F., 2006, "General temperature rise solution for a moving plane heat source problem in surface grinding", *Int. J. Adv. Manuf. Technol.* 31, 268-277.
- [26] Levin, P., 2008, "A general solution of 3-D quasi-steady-state problem of a moving heat source on a semi-infinite solid", *Mech. Research Communication* 35, pp. 151-157.
- [27] Yovanovich, M.M., 1974, "A general expression for predicting conduction shape factors," *AIAA, Thermophysics and Space Craft Control*, Vol. 35, pp. 265-291.
- [28] www.maplesoft.com, version 11.
- [29] Churchill, S.W. and Usagi, R., 1972, "A general expression for the correlation of rates of transfer and other phenomena", *AIChE Journal* 19, pp. 1121-1128.